Bioorganic & Medicinal Chemistry 17 (2009) 8093–8101

Contents lists available at ScienceDirect

Bioorganic & Medicinal Chemistry

journal homepage: www.elsevier.com/locate/bmc

The selective quantification of iron by hexadentate fluorescent probes

Yong Min Ma, Robert C. Hider *

Department of Pharmacy, King's College London, Franklin–Wilkins Building, 150 Stamford Street, London SE1 9NH, UK

ARTICLE INFO

Article history:
Received 1 September 2009
Revised 24 September 2009
Accepted 30 September 2009
Available online 8 October 2009

Keywords:
Fluorescence
Iron chelator
Non-transferrin-bound iron (NTBI)
Hexadentate

ABSTRACT

The synthesis of four hexadentate fluorescent probes is described, where the fluorescent moiety is based on either coumarin or fluorescein and the chelating moiety is based on either 3-hydroxypyridin-4-one or 3-hydroxypyran-4-one. The fluorescence is quenched when the probe chelating moieties bind iron. The probes were found to be selective for iron over other metals such as Cu, Zn, Ni, Mn and Co. The effect of Cu on fluorescence quenching can be eliminated in the presence of *N*,*N*,*N*′,*N*′-tetrakis(2-pyridylmethyl)-ethylenediamine. Competition studies demonstrate that the exchange of iron between pyridinone-based probes and apotransferrin is very slow. The ability to scavenge iron from oligomeric iron(III) citrate complexes demonstrate that the pyridinone probes scavenges iron faster than deferiprone and desferrioxamine. The fluorescence intensity of the fluorescein-based probe is quantitatively related to the iron concentration with the limit of detection being 10^{-8} M.

1. Introduction

Iron is one of the most important transition trace metals of all living cells. Iron overload, as well as iron deficiency, causes numerous health problems such as iron deficiency anemia, sickle cell anemia, thalassemia and hemochromatosis.[1,2] Such iron disorders can result from genetic defects, insufficient or excessive absorption of dietary iron or environmental factors.[3] Chemotherapy, exposure to toxic chemicals and natural body processes such as menstruation can all result in inappropriate distribution of body iron.[4] One parameter which changes with different body iron levels is non-transferrin bound iron (NTBI), the concentration of iron in the plasma which is not bound to transferrin.[5,6] At the present time there is no generally accepted method for the reliable measurement of the iron pool.[7,8] A wide range of methods have been investigated as possible means of making reliable NTBI measurements, such as the bleomycin assay,[9,10] inductively coupled plasma (ICP),[11,12] HPLC,[13] atomic absorption spectroscopy,[14,15] electrospray ionisation (ESI)[16] and fluorescence-based methods.[17–19] In this study, a fluorescent-based assay utilising hexadentate chelators is presented. The method is highly sensitive and relatively easy to use. The application to the measurement of NTBI is, however, limited by the variable autofluorescence of the serum samples.

2. Results and discussions

2.1. Design of the hexadentate fluorescent probes

In order to adopt the correct geometry of aromatic ligands for iron binding, it is essential that the backbone should be connected to the ring at the *ortho* position relative to one of the chelating oxygen atoms.[20] In this work, approaches to the design were made using an amide linkage located at either the 2- or 5-position of the 3-hydroxypyridin-4-one or the 2-position of the 3-hydroxypyran-4-one rings in order to direct the chelating oxygens to provide a suitable octahedral field to bind iron(III). In such examples, the amide group which links the ligands to the backbone structure is capable of forming an intramolecular hydrogen bond, resulting in a modified affinity of the corresponding iron complex (Fig. 1).[21]

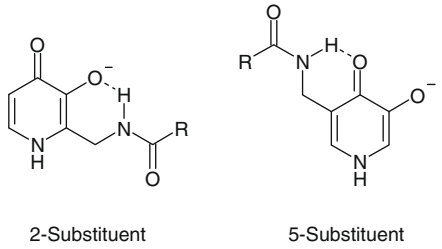

Figure 1. Intramolecular H-bond formation in *ortho* amido-3-hydrogypyridin-4-ones.

* Corresponding author. Tel.: +44 20 7848 4882; fax: +44 20 7848 4800.
E-mail address: robert.hider@kcl.ac.uk (R.C. Hider).

0968-0896/$ - see front matter © 2009 Elsevier Ltd. All rights reserved.
doi:10.1016/j.bmc.2009.09.052

2.2. Synthesis of the hexadentate fluorescent probes

The synthetic route of the three coumarin-based hexadentate probes is presented in Scheme 1. When amine **1**[22] was treated with coumarin **2**[23] in DMF in the presence of DCC/HOBt, the desired coumarin-linked triester **3** was furnished in good yield (65%). Hydrolysis of ester **3** to the triacid **4** was accomplished in 95% yield by treatment with formic acid. The coumarin-labelled triacid **4** was activated by reaction with DCC/NHS, then coupled with the aminopyridinones **5** or **6** or aminopyranone **7**[23] to furnish the corresponding protected fluorescent hexadentate molecules **8**–**10**. The protecting methyl or benzyl groups were removed by either treatment with BCl_3 or by hydrogenation to produce the desired iron-chelating probes **11**–**13**.

The synthesis of the fluorescein-labelled hexadentate ligand is outlined in Scheme 2. The protection of the amino group of β-alanine was achieved by treatment with *N*-ethyloxycarbonylphthalimide and sodium carbonate to give **14**, followed by coupling with amine **1** in DMF in the presence of DCC/HOBt to give a triester **15**. Deprotection of amino group in **15** by hydrazinolysis yielded amine **16**, which on coupling with fluorescein isothiocyanate produces the triester **17**. The triester was hydrolysed by formic acid to generate the triacid **18**. This acid was coupled to aminopyridinone **6** and de-protected using BCl_3 to yield the hexadentate probe **20**.

2.3. Fluorescence properties of the probes

The introduction of chelating moieties did not influence the λ_{max} of both the absorption and emission of the fluorescent hexadentate ligands. As shown in Table 1, the hexadentate probes have the same maximum absorption wavelength (λ_{abs}) and the same maximum emission wavelength (λ_{em}) as the parent molecule.

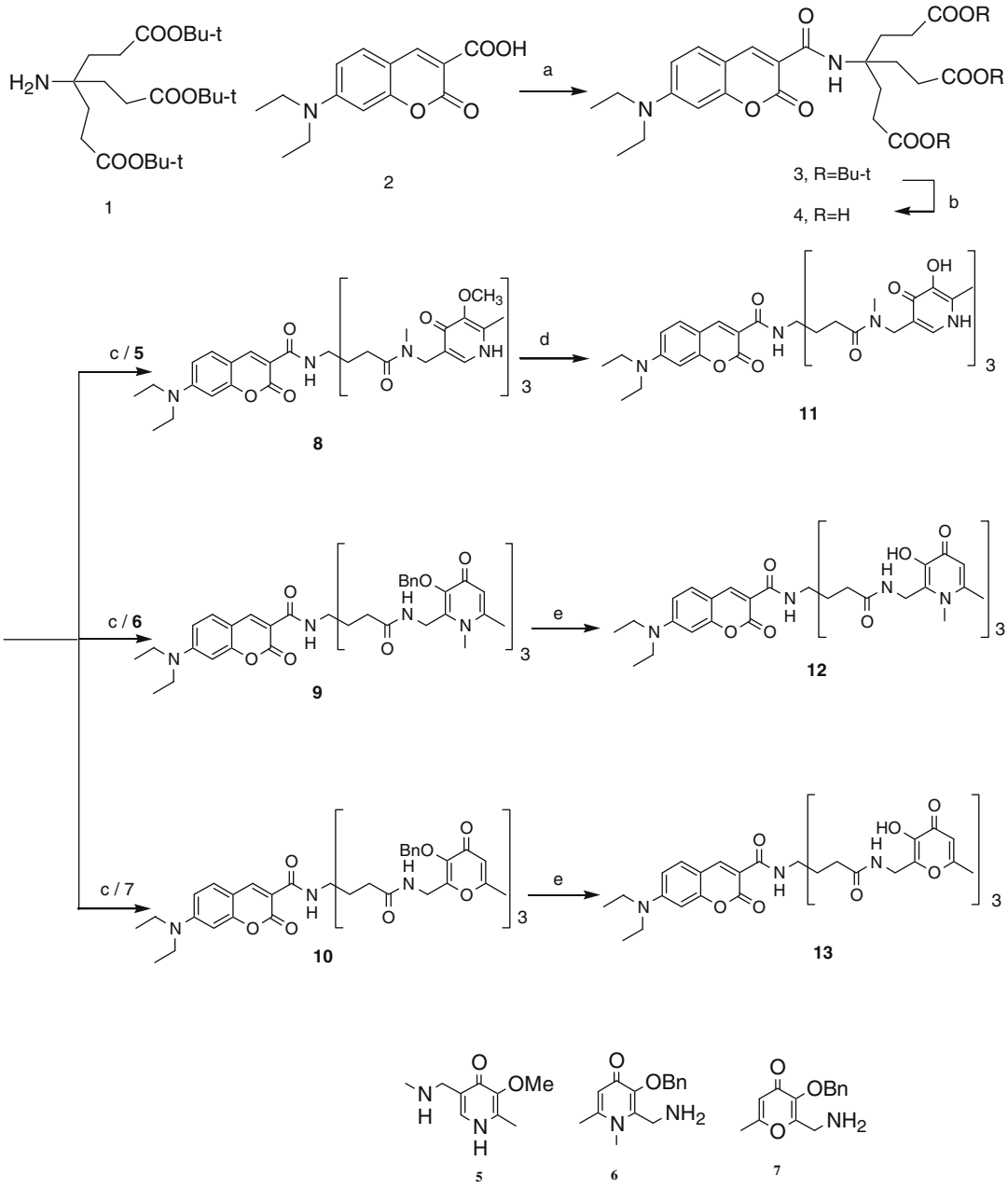

Scheme 1. Reagents and conditions: (a) DCC/HOBt, DMF, rt (65%); (b) HCOOH, rt 95%; (c) DCC/NHS, DMF, after 1 h followed by 3-methoxy-2-methyl-5-methylaminomethyl-1*H*-pyridin-4-one (**5**), 2-aminomethyl-3-benzyloxy-1,6-dimethyl-1*H*-pyridin-4-one (**6**) or 2-aminomethyl-3-benzyloxy-6-methyl-pyran-4-one (**7**), rt; (d) BCl_3, CH_2Cl_2; (e) Pd/C (cat.), H_2 2 bars, rt.

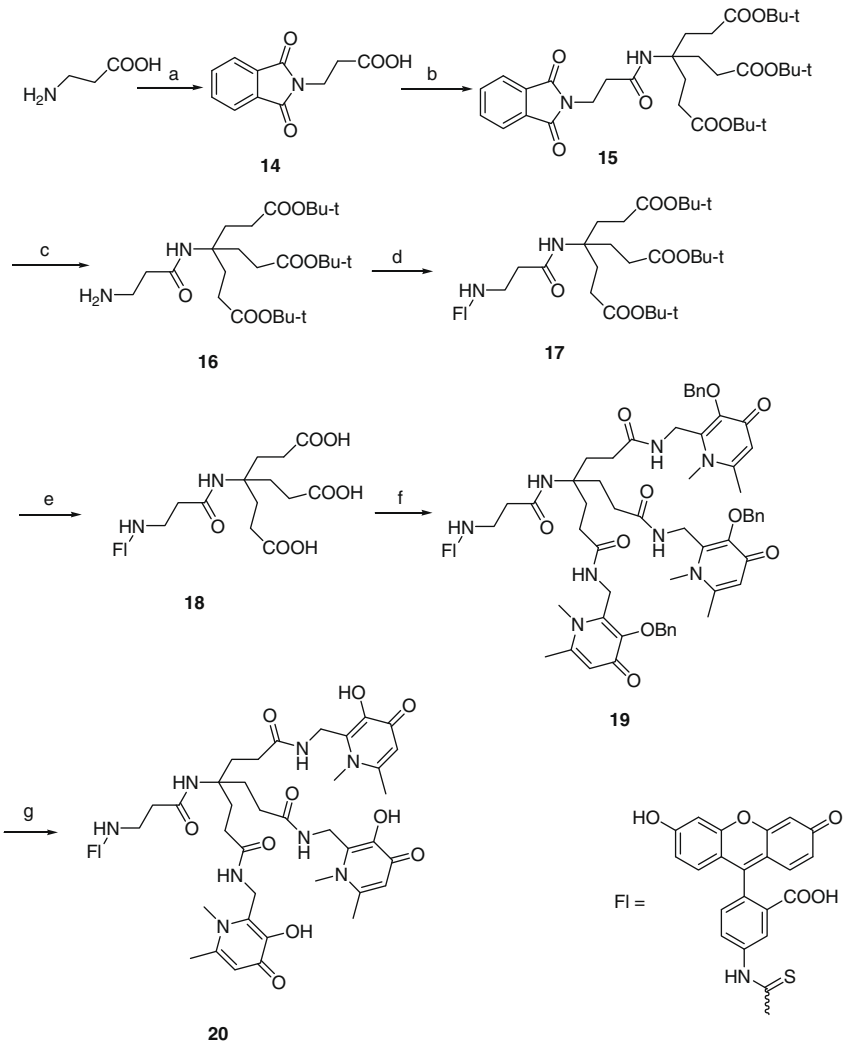

Scheme 2. Reagents and conditions: (a) *N*-ethyloxycarbonylphthalimide, Na_2CO_3, 72%; (b) DCC/HOBt, DMF, overnight, 66%; (c) NH_2NH_2, EtOH, 95%; (d) fluorescein isothiocyanate/DMF; (e) HCOOH, rt, 98%; (f) DCC/HOBt, 2-aminomethyl-3-benzyloxy-1,6-dimethyl-1*H*-pyridin-4-one (**6**), DMF; (g) BCl_3, CH_2Cl_2.

Table 1
Fluorescence characteristics of hexadentate probes

Code	λ_{abs} (nm)	λ_{em} (nm)
7-Diethylamino-coumarin-3-carboxylic acid	435	470
11	435	474
12	435	474
13	435	474
Fluorescein-5-isothiocyanate	494	519
20	494	513

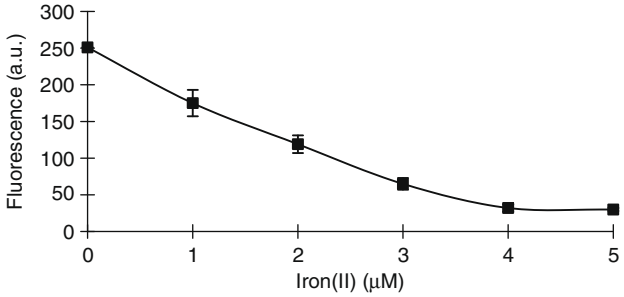

Figure 2. Fluorescence quenching of **11** by iron. The fluorescence intensity of **11** (6 μM) in MOPS (50 mM, pH 7.4) was measured by a Perkin–Elmer spectrofluorometer and recorded in arbitrary units (a.u.). The fluorescence intensity was then quenched by successive additions of iron using a ferrous ammonium sulfate (100 μM) stock solution.

The addition of iron does not result in either a red or blue shift of wavelength but does quench the fluorescence. Under ambient conditions, the hexadentate probe:iron-binding stoichiometry is predicted to be 1:1. In practice, the probes exceed the sensitivity predicted by their binding stoichiometry. Fluorimetric titrations of **11** demonstrate that the maximal quenching is reached at an iron:probe ratio of 0.67 (Fig. 2). Equivalent curves were obtained for each of the four probe molecules.

2.4. The Influence of different metals on the probe fluorescence

Although the hexadentate probes are selective for iron(III), they are also highly responsive to iron(II). This is because iron(II) is immediately oxidised after combining with the probes to form iron(III) complexes, due to its very high affinity for iron(III) (pFe^{III}–pFe^{II} >15; pFe is defined as the negative logarithm of the free iron concentration, calculated for a total ligand concentration of 10^{-5} M and a total iron concentration of 10^{-6} M at pH 7.4). Not only iron(II) and iron(III) but also other metals such as Cu(II), Co(II), Zn(II) were found to quench probe fluorescence. The relative quenching

potency of metals to **12** was found to be in the sequence Fe(III) ≈ Fe(II) > Cu(II) > Zn(II) > Ni(II) ≈ Mn(II) > Co(II) at a metal:probe ratio of 5:3 (Fig. 3). No quenching effect was observed with the following metal cations: Na, K, Ca and Mg (data not shown). All four compounds were found to behave in the same manner. The effect of Cu(II) on the quenching can be eliminated in the presence of the Cu(II) selective chelator *N*,*N*,*N*',*N*'-tetrakis(2-pyridylmethyl)-ethylenediamine (TPEN) (Fig. 3). The slope of fluorescence quenching by Zn(II) is higher than that of others, which demonstrates that although Zn(II) only partly quenches the probe fluorescence, it does bind to the probe and diminishes fluorescence quenching by iron(III).

2.5. Binding affinity of coumarin-labelled hexadentate probes

In order to investigate the relative iron affinities of the hexadentate probes, we studied their competition with nitrolotriacetic acid (NTA). NTA (0, 8 and 80 mM) was mixed with the coumarin-labelled hexadentate probes (6 μM) in tris-buffer (50 mM, pH 7.4) and the fluorescence quenching induced by the addition of iron(II) (6 μM) was recorded. The presence of NTA did not influence the fluorescence quenching of **12** on addition of iron (Fig. 4). In contrast, the fluorescence quenching of **13** by iron was markedly affected in the presence of 8 mM NTA. The higher the NTA concentration, the less probe quenching occurs. This finding is consistent with the prediction that a pyridinone hexadentate chelator will possess a higher affinity for iron than a pyranone counterpart.[24] Surprisingly, the fluorescence quenching of **11**, another pyridinone hexadentate probe, was also found to be dependent on the NTA concentration (Fig. 4). This may result from a lack of an intramolecular hydrogen bond with 3-hydroxy group, which leads to a higher pK_{a_2} value (3-hydroxy group) and correspondingly a lower iron affinity compared to that of **12**. Based on these competition studies, the metal affinity sequence of the three probes is: **12** > **11** > **13**. This result was confirmed in other competition studies using non-fluorescent chelators such as maltol (1 mM), deferiprone (1 mM) and desferrioxamine (DFO; 6 μM) (data not shown).

2.6. Iron quantification

Using 6 μM coumarin-labelled probes, the iron concentration can be determined over the range 0.5–3 μM. The lower the probe concentration, the lower the iron concentration which can be quantified. However, due to the low molar extinction coefficient and low quantum yield, coumarin-labelled probes have limited sensitivity in such measurements. In order to enhance the sensitivity, a fluorescein derivative was also investigated, as fluorescein has a much higher molar extinction coefficient and quantum yield. Furthermore, fluorescein has a higher emission λ_{max} value and therefore experiences a reduced interference from biological samples. Thus the probe **20**, at a concentration of 50 nM, was used to investigate the quenching by iron(III). The fluorescence decreased correspondingly and a linear curve was obtained (Fig 5). Using this system, iron can be reliably quantified down to levels of 10 nM.

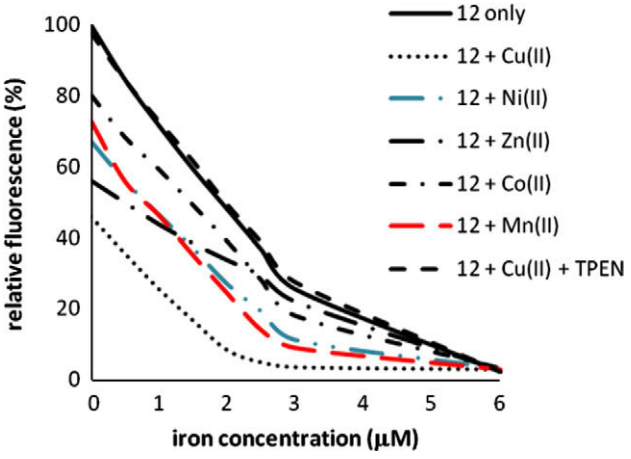

Figure 3. Fluorescence quenching of **12** by iron(III) in the presence of various metals. The initial fluorescence of **12** (6 μM) in MOPS (50 mM, pH 7.4) was set at 100% relative fluorescence. The fluorescence of probe in the presence of various metals (10 μM) was expressed as percentage of initial fluorescence. The fluorescence intensity was then decreased by successive additions of iron(III) (100 μM stock solution) prepared from $FeCl_3$ and NTA (1:2.2 molar ratio). The metal ions were prepared from their corresponding salts ($CuCl_2$, $NiCl_2$, $ZnCl_2$, $CoCl_2$ and $MnCl_2$).

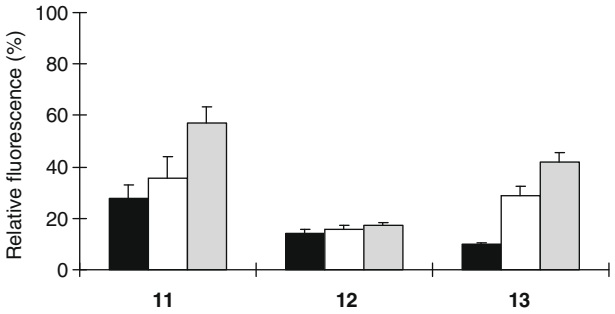

Figure 4. The effect of concentration of NTA on the fluorescence quenching of hexadentate fluorescent probes. The fluorescence of **11–13** (6 μM) in MOPS (50 mM, pH 7.4) in the presence of different concentrations of NTA was recorded at λ_{ex} = 435 nm and λ_{em} = 477 nm and set at 100% relative fluorescence. After the addition of iron(II) (6 μM), the fluorescence of the mixture was measured using the same instrument settings. The black, white and grey bars are expressed in the presence of NTA at 0, 8 and 80 mM, respectively.

2.7. Competition between the hexadentate probes and chelators present in serum

Solutions of monoiron-transferrin were mixed with partially iron-chelated fluorescent probes and the fluorescence of the resulting solution was monitored every few hours. The fluorescence of the solutions containing transferrin/**11**/iron and transferrin/**12**/iron were found to gradually decrease with time (Fig. 6). The opposite effect occurred with transferrin/**13**/iron (Fig. 6). This is due to higher metal affinities of **11** and **12** than that of transferrin, which leads to iron redistribution from transferrin to the probe. In contrast, **13**, with the hydroxypyranone chelating unit, has a weaker iron affinity constant and thus it transfers iron to transferrin. The

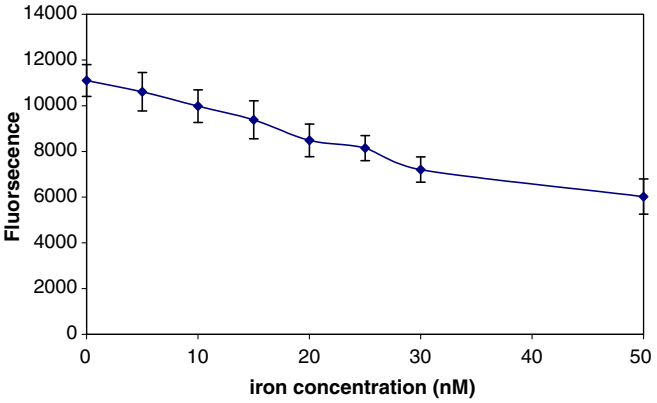

Figure 5. Fluorescence quenching of **20** by iron(III). The fluorescence intensity of **20** (50 nM) and various concentrations of iron(III) in MOPS (50 mM, pH 7.4) was measured at 494/513 nm excitation/emission and presented in arbitrary units.

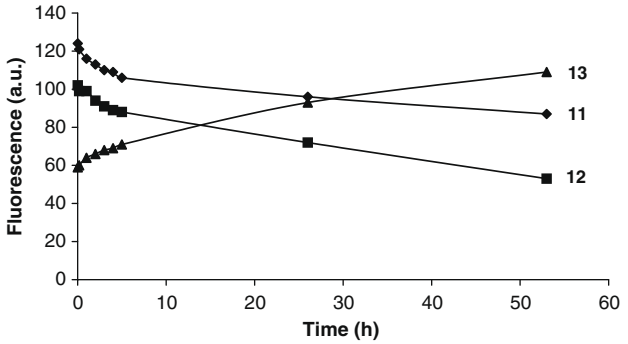

Figure 6. Competition of iron(III) between transferrin and hexadentate probes **11**, **12** and **13**. Monoferric transferrin (65 μM) was prepared from apotransferrin and $Fe(NTA)_2$, both the final concentration at 65 μM, in $NaHCO_3$ (50 mM, pH 8.0) and the solution was incubated at 37 °C for 1 h before use. Half-full iron-chelated probes (12 μM) was prepared from fluorescent probes (12 μM) and $Fe(NTA)_2$ (6 μM) in MOPS (50 mM, pH 7.4). Equal volumes of mono-transferrin and half-full iron-chelated probes were mixed and the fluorescence was measured immediately and continually at 435/474 nm excitation/emission using a spectrofluorometer for 53 h.

rates of iron exchange under these conditions were relatively slow, relatively little exchange occurring after 30 min.

Citrate, a potential iron-binding ligand, combines with iron to form many complexes including oligomeric complexes with molecular masses in the range 1.5–5 kDa.[25] It is important to investigate the competition of the probes with iron-citrate complexes as they are major components of NTBI.[26] Iron citrate solution was prepared at pH 7.4 to final concentrations of 10 μM iron and 100 μM citrate. Four iron ligands, CP20, DFO, **12** and **13**, were selected to investigate the rate of scavenging oligomeric iron. DFO, a highly hydrophilic hexadentate ligand, has been reported to chelate oligomeric iron citrate by a relatively slow process.[27] This report is consistent with our own observations; the observed $T_{1/2}$ value of this competition process was 92 min (Fig. 7). Compared to DFO, CP20 was found to have a shorter $T_{1/2}$ value (15 min). Not surprisingly, **12**, the hexadentate pyridinone ligand, was found to exchange iron at the fastest rate ($T_{1/2}$ = 9 min). The hexadentate pyranone (**13**) was associated with the slow exchange rate of 46 min (Fig. 7). Moreover, the pyranone ligand failed to scavenge all iron from this iron citrate solution, even after 24 h.

2.8. NTBI quantification

NTBI levels fall into the range of 0–15 μM.[19,28] In order to develop a reliable quantitative method, we have investigated the most promising probes **12** and **20**. Iron (0–1 μM final concentration) was added to a MOPS buffer containing 2 μM **12** at pH7.4 after 10 min, followed by an addition of serum (10% for final percentage). The fluorescence of the mixture was then measured and calculated as a percentage of the initial fluorescence in which no iron was added. The difference of the fluorescence between probe only and probe with various iron additions is calculated as Δ*F*. With the increase of iron added, Δ*F* increases correspondingly. A linear standard curve was obtained (Fig. 8a). Referring to the standard curves, 'unknown' samples (0–10 μM, prepared blind by other member of the research group) were performed under the same experimental conditions and the iron concentrations were calculated. If necessary, the 'unknown' iron solution is diluted to allow the Δ*F* value to fall in the range 0–0.9. The measured iron concentrations of the 'unknown' samples using the probe **12** demonstrated good agreement with their known iron content (Table 2).

However, when the probe **12** was applied for the determination of NTBI in iron-overloaded patients using a multiwell plate reader, it was found to be difficult to quantify the NTBI concentration in the range of 0–10 μM for two reasons. One, there were no suitable excitation/emission filters which matched the maximum excitation/emission wavelength of the probe (λ_{ex} = 435 nm, λ_{em} = 474 nm). This decreased the sensitivity of the fluorescence method. The second reason is that due to the comparatively low excitation/emission wavelengths, the autofluorescence from the serum influences the sample fluorescence determination to an appreciable extent, which leads to false readings. In principle the

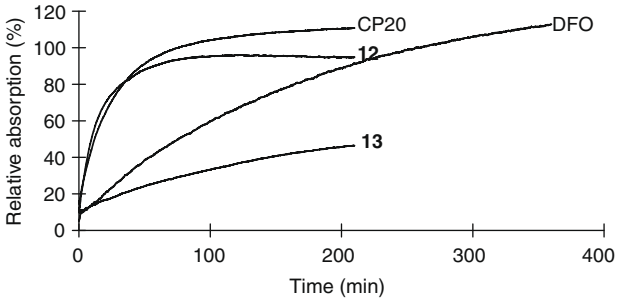

Figure 7. The comparison of several iron ligands chelating oligomeric iron. The absorption of CP20 (30 μM) and $Fe(NTA)_2$ (10 μM) was measured at 460 nm and set at 100% relative absorption. The absorption of CP20 (30 μM) in the presence of oligomeric iron (10 μM) was measured at same wavelength and given as a percentage of that of CP20–$Fe(NTA)_2$ complex. The absorption of DFO, **12** and **13** (10 μM each) in the presence of oligomeric iron (10 μM) was measured at 430, 475 and 475 nm, respectively in a time-course and expressed as a percentage of the absorption of these ligands with $Fe(NTA)_2$ (10 μM) at each respective wavelength.

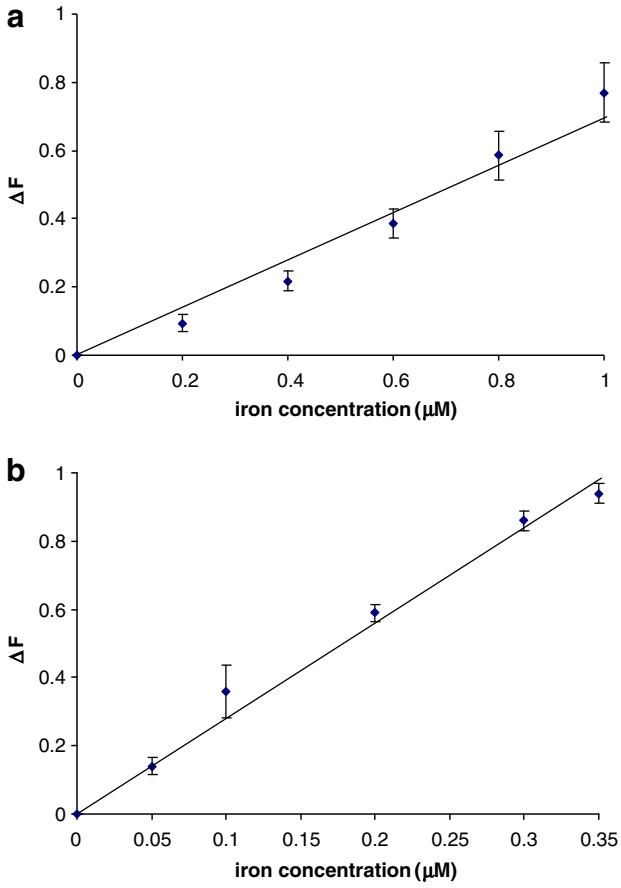

Figure 8. Standard curves of the fluorescence quenching of **12** (a) and **20** (b) by additions of various concentrations of iron. The initial fluorescence of **12** (2 μM) or **20** (0.5 μM) in MOPS (50 mM) at pH 7.4 in the presence of 10% serum was set at 100% and the relative fluorescence of the mixtures of the probe and various concentrations of iron was calculated and the difference of the fluorescence between the probe–iron mixtures and probe only is presented as Δ*F*.

Table 2
Comparison of 'unknown' iron concentrations with measured concentrations in 10% serum determined by **12** and **20** ($n = 4$)

'Unknown' [iron]	Measured [iron] with **12**	'Unknown' [iron]	Measured [iron] with **20**
4	3.9 ± 0.2	9.5	9.05 ± 0.18
0	0.3 ± 0.2	8.2	8.66 ± 0.08
6	5.7 ± 0.3	7	8.22 ± 0.08
1	1.4 ± 0.2	6.8	7.63 ± 0.11
2	2.3 ± 0.1	4.9	5.63 ± 0.22
10	9.6 ± 0.7	3.2	3.32 ± 0.18
5	5.1 ± 0.3	2.5	2.92 ± 0.24
8	7.9 ± 0.6	1.4	1.79 ± 0.50
7	7.4 ± 0.4	0	−0.02 ± 0.13
3	3.4 ± 0.2		
9	9.0 ± 0.5		

use of the fluorescein-based hexadentate probe **20** could minimise these problems. The fluorescence of 0.5 μM **20** was measured by a 96-well plate reader (Ex: 485 ± 20 nm; Em: 530 ± 25 nm) and a standard curve was constructed in similar fashion to that described for **12** (Fig. 8b). The iron concentrations of 'unknown' samples were then calculated according to the standard curve. Again, the measured iron concentrations are comparable to the known iron content (Table 2).

Interestingly, when serum (10% dilution) was incubated with various iron levels for 30 min before adding the probe **20**, a linear relationship was not obtained between the 'unknown' iron level and measured iron (Fig. 9). Over the range 0–4 μM, the iron concentration was recorded at the same level, that is, approximately 0 μM. This is a result of the presence of apotransferrin in the serum sample which chelates added iron until saturated. The probe is not able to scavenge iron from transferrin in the adopted experimental time. When all the apotransferrin is saturated with iron, additional iron is available to be measured by the probe. Therefore, a linear curve is observed over the range of 4–8 μM added iron concentration (Fig. 9). Using this method, the percentage saturation of transferrin can be calculated.

Unfortunately, when this direct method was applied to various serum samples, the resulting NTBI concentrations were found to vary and were not comparable to those determined by the HPLC method.[13] The colour and autofluorescence varies between different serum samples and this has a major influence on the results. As this fluorescence method is so sensitive (only 0.5 μM of probe is used in this study), any small change of fluorescence including autofluorescence from the serum leads to a relatively large change in fluorescence emission.

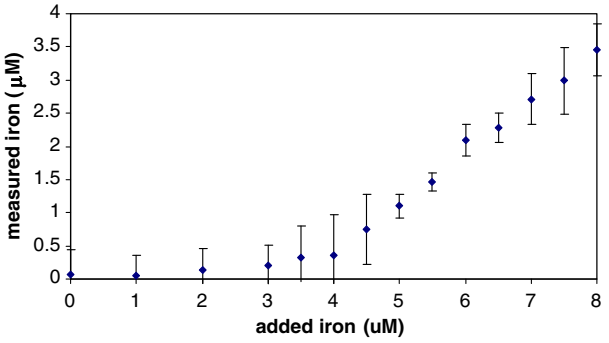

Figure 9. The relationship of concentrations between added iron and measured iron by **20**. The fluorescence of **20** (0.5 μM) in a mixture of 10% serum with various concentrations of iron was measured by a 96-well plate reader. The difference of the fluorescence between probe-serum-iron complex and probe-serum only was calculated and converted to iron concentration according to the standard curve of **20**.

3. Conclusion

Four hexadentate fluorescent probes have been described, three based on the coumarin moiety and one on fluorescein. These probes were found to be more selective for iron than other bivalent metals such as Cu, Zn, Ni, Mn and Co. Although Cu has a marked effect on the fluorescence quenching, the contribution of this metal in our study is likely to be negligible due to its relatively low concentration in serum. Furthermore, should competition by copper be a problem it can be abolished by the inclusion of TPEN in the assay. Iron affinity studies show that the pyridinone-based hexadentates are capable of competing all iron from weak ligands such as NTA and citrate. By increasing the molar extinction coefficient and quantum yield of the fluorophore, the detection limit of iron concentration has been decreased to 10 nM. However, neither coumarin- nor fluorescein-based probes are suitable for the direct determination of NTBI, due to the variable color and autofluorescence of sera. We continue to seek a reliable fluorescence-based method for the quantification of NTBI.

4. Experimental

4.1. General

All chemicals were purchased from commercial sources and used without further purification. Normal mixed pool serum was purchased from First Link (UK) Ltd. Melting points were determined using an Electrothermal IA 9100 Digital Melting Point Apparatus and are uncorrected. ^{1}H NMR spectra were recorded using a Bruker (360 MHz) NMR spectrometer. Chemical shifts (δ) are reported in ppm downfield from the internal standard tetramethylsilane (TMS). Mass spectra (FAB) analyses were carried out by the Mass Spectrometry Facility, School of Health and Life Science, King's College London. Elemental analyses were performed by Micro-analytical laboratories, Department of Chemistry, The University of Manchester.

4.1.1. 7-Diethylamino-*N*-[(tri-*tert*-butoxycarbonylethyl)methyl]-2-oxo-*2H*-chromen-3-carboxamide (3)

A mixture of di-*tert*-butyl 4-amino-4-[2-(*tert*-butoxycarbonyl)ethyl] heptanedioate **1** (10 mmol), 7-diethylamino-2-oxo-*2H*-chromen-3-carboxylic acid **2** (10 mmol), dicyclohexylcarbodiimide (DCC, 12 mmol), 1-hydroxybenzotriazole (HOBt, 10 mmol), and DMF (100 mL) was stirred at room temperature overnight. After filtration and removal of the solvent under reduced pressure, the residue was chromatographed on silica gel using MeOH/$CHCl_3$ (1:9) as an eluent to afford a yellow solid (65%). Mp 196–197 °C; ^{1}H NMR ($CDCl_3$) δ: 1.24 (t, J = 7.1 Hz, CH_3CH_2N, 6H), 1.43 (s, $C(CH_3)_3$, 27H), 2.06–2.10 (m, CH_2CH_2CO, 6H), 2.23–2.28 (m, CH_2CH_2CO, 6H), 3.46 (q, J = 7.1 Hz, CH_3CH_2N, 4H), 6.50 (d, J = 2.3 Hz, courmain C-8H, 1H), 6.64 (dd, J = 2.4, 9.0 Hz, courmain C-6H, 1H), 7.39 (d, J = 9.0 Hz, courmain C-5H, 1H), 8.65 (s, courmain C-4H, 1H). ESI-MS: 659 $(M+1)^+$.

4.1.2. 7-Diethylamino-*N*-[(tri-(2-carboxylethyl)methyl]-2-oxo-*2H*-chromen-3-carboxamide (4)

A solution of the *tert*-butyl ester **3** (10 mmol) in formic acid (96%, 10 mL) was stirred at 25 °C overnight. After concentration, toluene (5 mL) was added and the solution was again evaporated in vacuo to remove azeotropically any residual formic acid. The residue was then precipitated in acetone (50 mL) to afford a yellow solid (95%), which can be used for the next step without further purification. Mp 144–146 °C; ^{1}H NMR ($CDCl_3$) δ: 1.24 (t, J = 7.1 Hz, CH_3CH_2N, 6H), 1.94–1.98 (m, CH_2CH_2CO, 6H), 2.21–2.26 (m, CH_2CH_2CO, 6H), 3.45 (q, J = 7.1 Hz, CH_3CH_2N, 4H), 6.51 (d,

J = 2.3 Hz, courmain C-8H, 1H), 6.63 (dd, *J* = 2.4, 9.0 Hz, courmain C-6H, 1H), 7.39 (d, *J* = 9.0 Hz, courmain C-5H, 1H), 8.64 (s, courmain C-4H, 1H). ESI-MS: 491 $(M+1)^+$.

4.1.3. 7-Diethylamino-*N*-{[tri-(2-{*N*-[(5-methoxy-6-methyl-4-oxo-1,4-dihydropyridin-3-yl)methyl]-*N*-methylcarbamoyl}ethyl)]methyl}-2-oxo-*2H*-chromen-3-carboxamide (8)

To a solution of compound **4** (10 mmol) in dry DMF (100 mL), DCC (12 mmol) and *N*-hydroxysuccinimide (NHS) (12 mmol) were added. The mixture was allowed to stir for 2 h before 3-methoxy-2-methyl-5-methylaminomethyl-*1H*-pyridin-4-one **5** (10 mmol) was added, and the reaction was left to stir at room temperature overnight. The precipitation was removed by filtration, and the solvent was evaporated. The residue was dissolved in dichloromethane and washed with 0.1 N NaOH (3×) and brine, dried over anhydrous Na_2SO_4 and concentrated under reduced pressure, The obtained residue was purified by column chromatography ($MeOH/CHCl_3$, 1:9), affording the title compound as a yellow solid (Yield 59%). Mp 206–209 °C; ^1H NMR ($CDCl_3$) δ: 1.14 (t, *J* = 7.1 Hz, CH_3CH_2N, 6H), 1.92–2.09 (m, CH_2CH_2CO, 6H), 2.18 (s, CCH_3, 9H), 2.32–2.42 (m, CH_2CH_2CO, 6H), 3.06 (s, NCH_3, 9H), 3.47 (q, *J* = 7.4 Hz, CH_3CH_2N, 4H), 3.79 (s, OCH_3, 9H), 4.46 (s, CCH_2N, 6H), 6.50 (d, *J* = 2.0 Hz, courmain C-8H, 1H), 6.67 (dd, *J* = 2.0, 9.0 Hz, courmain C-6H, 1H), 7.42 (d, *J* = 9.1 Hz, courmain C-5H, 1H), 8.57 (s, courmain C-4H, 1H), 8.61 (s, pyridinone C-6H, 3H). ESI-MS: 983 $(M+1)^+$. Elemental Anal. Calcd for $C_{51}H_{66}N_8O_{12}\cdot CHCl_3\cdot 7H_2O$: C, 50.84; H, 6.65; N, 9.12. Found: C, 50.70; H, 6.44; N, 9.31.

Analogous procedures starting with triacid **4** with 2-aminomethyl-3-benzyloxy-1,6-dimethyl-1*H*-pyrindin-4-one **6** or 2-aminomethyl-3-benzyloxy-6-methyl-pyran-4-one **7** gave compounds **9** and **10**, respectively.

4.1.4. 7-Diethylamino-*N*-{[tri-(2-{*N*-[(3-benzoxy-1,6-dimethyl-4-oxo-1,4-dihydropyridin-2-yl)methyl]carbamoyl}ethyl)]methyl}-2-oxo-*2H*-chromen-3-carboxamide (9)

Mp 231–232 °C; ^1H NMR ($CDCl_3$) δ: 1.25 (t, *J* = 7.1 Hz, CH_3CH_2N, 6H), 2.05–2.10 (m, CH_2CH_2CO, 6H), 2.13 (s, CCH_3, 9H), 2.15–2.21 (m, CH_2CH_2CO, 6H), 3.36 (s, NCH_3, 9H), 3.44 (q, *J* = 7.1 Hz, CH_3CH_2N, 4H), 4.29 (d, *J* = 5.3 Hz, CCH_2N, 6H), 4.95 (s, $PhCH_2O$, 6H), 6.14 (s, pyridinone C-5H, 3H), 6.47 (d, *J* = 2.2 Hz, courmain C-8H, 1H), 6.65 (dd, *J* = 2.3, 9.1 Hz, courmain C-6H, 1H), 6.73 (br s, NH, 3H), 7.22–7.30 (m, PhH, 15H), 7.39 (d, *J* = 9.0 Hz, courmain C-5H, 1H), 8.60 (s, courmain C-4H, 1H). ESI-MS: 1211 $(M+1)^+$. Elemental Anal. Calcd for $C_{69}H_{78}N_8O_{12}$: C, 68.41; H, 6.49; N, 9.25. Found: C, 68.08; H, 6.43; N, 9.46.

4.1.5. 7-Diethylamino-*N*-{[tri-(2-{*N*-[(3-benzoxy-6-dimethyl-4-oxo-*4H*-pyran-2-yl)methyl]carbamoyl}ethyl)]methyl}-2-oxo-*2H*-chromen-3-carboxamide (10)

Mp 169–171 °C; ^1H NMR ($CDCl_3$) δ: 1.25 (t, *J* = 7.0 Hz, CH_3CH_2N, 6H), 2.06 (br s, CH_2CH_2CO, 12H), 2.20 (s, CCH_3, 9H), 3.46 (q, *J* = 7.0 Hz, CH_3CH_2N, 4H), 4.13 (d, *J* = 5.9 Hz, CCH_2N, 6H), 5.16 (s, $PhCH_2O$, 6H), 5.63 (q, *J* = 5.9 Hz, NH, 3H), 6.15 (s, pyridinone C-5H, 3H), 6.49 (s, courmain C-8H, 1H), 6.66 (d, *J* = 9.0 Hz, courmain C-6H, 1H), 7.31–7.35 (m, PhH, 15H), 7.40 (d, *J* = 9.0 Hz, courmain C-5H, 1H), 8.60 (s, courmain C-4H, 1H), 8.63 (s, NH, 1H). ^{13}C NMR (100 MHz, $CDCl_3$) δ: 12.42 (CH_3), 19.66 (CH_3), 30.55 (CH_2), 30.76 (CH_2), 36.24 (CH_2), 45.15 (CH_2), 58.17 (C), 73.58 (CH_2), 96.50 (CH), 108.28 (C), 109.78 (C), 110.30 (CH), 114.93 (CH), 128.69 (CH), 129.50 (CH), 131.31 (CH), 136.58 (C), 142.43 (C), 148.01 (CH), 152.92 (C), 156.48 (C), 157.74 (C), 162.37 (C), 163.12 (C), 164.80 (C), 172.42 (C), 175.82 (C). ESI-MS: 1172 $(M+1)^+$. Elemental Anal. Calcd for $C_{66}H_{69}N_5O_{15}\cdot 0.5CHCl_3$: C, 64.83; H, 5.69; N, 5.68. Found: C, 64.45; H, 5.84; N, 5.65.

4.1.6. 7-Diethylamino-*N*-{[tri-(2-{*N*-[(5-hydroxy-6-methyl-4-oxo-1,4-dihydropyridin-3-yl)methyl]-*N*-methylcarbamoyl}ethyl)]methyl}-2-oxo-*2H*-chromen-3-carboxamide (11)

A solution of compound **8** (3 mmol) in CH_2Cl_2 (50 ml) was flushed with nitrogen. After the flask was cooled to 0 °C, boron trichloride (1 M in CH_2Cl_2, 20 ml) was added dropwise and the reaction mixture was allowed to stir at room temperature for 1 d. The excess BCl_3 was eliminated at the end of the reaction by the addition of methanol (10 ml) and left to stir for another 10 min. After removal of the solvents under reduced pressure, the residue were purified by recrystallization from methanol/acetone to afford yellow solid (77%). Mp 173–175 °C; ^1H NMR (400 MHz, CD_3OD) δ: 1.26 (t, *J* = 7.0 Hz, CH_3CH_2N, 6H), 2.16–2.22 (m, CH_2CH_2CO, 6H), 2.35–2.61 (2 m, CH_2CH_2CO, 6H), 2.53 and 2.55 (2s, CCH_3, 9H), 2.78 and 3.20 (2s, NCH_3, 9H), 3.55 (q, *J* = 7.0 Hz, CH_3CH_2N, 4H), 4.27 and 4.57 (2s, CCH_2N, 6H), 6.56 (s, courmain C-8H, 1H), 6.85 (d, *J* = 8.3 Hz, courmain C-6H, 1H), 7.53 (d, *J* = 8.3 Hz, courmain C-5H, 1H), 8.15 and 8.16 (2s, pyridinone C-6H, 3H), 8.51 (s, courmain C-4H, 1H). ^{13}C NMR (100 MHz, CD_3OD) δ: 12.73 (CH_3), 14.30 and 14.51 (CH_3), 28.46 (CH_2), 29.28 (CH_2), 31.06 (CH_2), 33.54 (CH_3), 36.78 (CH_3), 46.10 (CH_2), 46.39 and 46.65 (CH_2), 59.15 (C), 97.34 (CH), 111.86 (CH), 121.99 (C), 132.72 (CH), 135.05 and 136.64 (CH), 141.41 (C), 144.27 (C), 148.94 (CH), 154.65 (C), 159.20 (C), 160.35 (C), 164.48 (C), 165.50 (C), 176.86 (C), 177.88 (C). ESI-MS: 941 $(M+1)^+$. Elemental Anal. Calcd for $C_{49}H_{71}N_8O_{15}Cl_5$: C, 49.48; H, 6.02; N, 9.42. Found: C, 49.94; H, 6.18; N, 9.55.

4.1.7. 7-Diethylamino-*N*-{[tri-(2-{*N*-[(3-hydroxy-1,6-dimethyl-4-oxo-1,4-dihydropyridin-2-yl)methyl]carbamoyl}ethyl)]methyl}-2-oxo-*2H*-chromen-3-carboxamide (12)

A solution of compound **9** (5 mmol) in ethanol (30 ml) was subjected to hydrogenolysis in presence of 5% Pd/C (w/w) catalyst overnight. The catalysts were removed by filtration and the filtrates were acidified to pH 1 with concentrated hydrochloric acid. After removal of the solvents in vacuo, the residues were purified by recrystallization from methanol/acetone to afford a yellow solid (87%). Mp 195–196 °C; ^1H NMR (360 MHz, CD_3OD) δ: 1.26 (t, *J* = 6.4 Hz, CH_3CH_2N, 6H), 2.12 (s, CH_2CH_2CO, 6H), 2.33 (s, CH_2CH_2CO, 6H), 2.65 (s, CCH_3, 9H), 3.56 (q, *J* = 6.4 Hz, CH_3CH_2N, 4H), 4.02 (s, NCH_3, 9H), 4.72 (s, CCH_2N, 6H), 6.56 (s, courmain C-8H, 1H), 6.86 (d, *J* = 8.6 Hz, courmain C-6H, 1H), 7.07 (s, pyridinone C-5H, 3H), 7.53 (d, *J* = 8.6 Hz, courmain C-5H, 1H), 8.48 (s, courmain C-4H, 1H). ^{13}C NMR (100 MHz, CD_3OD) δ: 12.74 (CH_3), 21.25 (CH_3), 30.70 (CH_2), 31.35 (CH_2), 36.56 (CH_2), 39.92 (CH_3), 46.06 (CH_2), 59.25 (C), 97.22 (CH), 109.44 (C), 110.38 (C), 111.90 (CH), 114.23 (CH), 132.74 (CH), 140.93 (C), 144.82 (C), 148.90 (CH), 150.81 (C), 154.72 (C), 159.10 (C), 161.36 (C), 164.21 (C), 164.37 (C), 176.50 (C). ESI-MS: 941 $(M+1)^+$. Elemental Anal. Calcd for $C_{48}H_{73}N_8O_{17}Cl_3$: C, 50.55; H, 6.45; N, 9.82. Found: C, 50.95; H, 6.49; N, 9.62.

4.1.8. 7-Diethylamino-*N*-{[tri-(2-{*N*-[(3-hydroxy-6-dimethyl-4-oxo-*4H*-pyran-2-yl)methyl]carbamoyl}ethyl)]methyl}-2-oxo-*2H*-chromen-3-carboxamide (13)

An analogous procedure starting with compound **10** gave 7-diethylamino-*N*-{[tri-(2-{*N*-[(3-hydroxy-6-dimethyl-4-oxo-*4H*-pyran-2-yl)methyl]carbamoyl}ethyl)]methyl}-2-oxo-*2H*-chromen-3-carboxamide (**13**). Mp 139–141 °C; ^1H NMR (DMSO-d_6) δ: 1.16 (t, *J* = 7.0 Hz, CH_3CH_2N, 6H), 1.93–1.99 (m, CH_2CH_2CO, 6H), 2.16–2.19 (m, CH_2CH_2CO, 6H), 2.27 (s, CCH_3, 9H), 3.46 (q, *J* = 7.1 Hz, CH_3CH_2N, 4H), 4.54 (d, *J* = 5.8 Hz, CCH_2N, 6H), 6.24 (s, pyridinone C-5H, 3H), 6.64 (d, *J* = 1.9 Hz, courmain C-8H, 1H), 6.85 (dd, *J* = 2.0, 9.1 Hz, courmain C-6H, 1H), 7.76 (d, *J* = 9.1 Hz, courmain C-5H, 1H), 8.60 (s, courmain C-4H, 1H), 8.99 (t, *J* = 5.8 Hz, NH, 3H). ESI-MS: 902 $(M+1)^+$.

4.1.9. 3-(1,3-Dioxoisoindolin-2-yl)propanoic acid (14)

A vigorously stirred solution of β-analine (4.46 g, 50 mmol) and sodium carbonate (5.35 g, 50.5 mmol) in water (100 mL) was treated with *N*-ethyloxycarbonylphthalimide (11.51 g, 52.5 mmol) and stirred for 1 h. The solution was filtered and the residue was acidified to pH 2–3 with 6 N HCl, which resulted in a white precipitate. The solution was filtered and the precipitate was washed with water and drying in air to obtain a white crystal (7.89 g, 72% yield). Mp 150–152 °C (lit[29] 152–153 °C). ^{1}H NMR (DMSO-d_6) δ: 2.61 (t, J = 7.3 Hz, CH_2CO, 2H), 3.80 (t, J = 7.3 Hz, NCH_2, 2H), 7.82–7.89 (m, ArH, 4H).

4.1.10. Di-*tert*-butyl 4-(2-(*tert*-butoxycarbonyl)ethyl)-4-(3-(1,3-dioxoisoindolin-2-yl)propanamido)heptanedioate (15)

A mixture of **14** (2.19 g, 10 mmol), amine **1** (4.57 g, 11 mmol), DCC (2.27 g, 11 mmol), HOBt (1.49 g, 11 mmol) in DMF (60 mL) was stirred at room temperature for 1 d. After filtration, the solvent was removed under reduced pressure, the residue was purified on a silica gel column using EtOAc/MeOH (9.5:0.5) as an eluent to afford a white solid (4.08 g, 66%). Mp 144–145 °C. ^{1}H NMR ($CDCl_3$) δ: 1.43 (s, $C(CH_3)_3$, 27H), 1.93–1.98 (m, CH_2CH_2CO, 6H), 2.18–2.23 (m, CH_2CH_2CO, 6H), 2.56 (t, J = 7.5 Hz, CH_2CO, 2H), 3.97 (t, J = 7.5 Hz, NCH_2, 2H), 6.13 (s, NH, 1H), 7.71 (m, ArH, 2H), 7.85 (m, ArH, 2H). ESI-MS: 617 $(M+1)^+$.

4.1.11. Di-*tert*-butyl 4-(2-(*tert*-butoxycarbonyl)ethyl)-4-(3-amino)propanamido)heptanedioate (16)

To a solution of **15** (3 mmol) in ethanol (40 mL) was added 5.5% aqueous hydrazine (3 mL). After being refluxed for 3 h, the reaction mixture was cooled to 0 °C, acidified to pH 1 with concentrated HCl, and filtered. The filtrate was concentrated in vacuo, and the residue was dissolved in distilled water (40 mL), adjusted to pH 12 with 10 N NaOH, and extracted with chloroform (5 × 100 mL). The combined organic extracts were dried over anhydrous Na_2SO_4 under reduced pressure to furnish **16** (85%) as pale brown oil. ^{1}H NMR ($CDCl_3$) δ: 1.43 (s, $C(CH_3)_3$, 27H), 1.94–1.99 (m, CH_2CH_2CO, 6H), 2.19–2.24 (m, CH_2CH_2CO, 6H), 2.29 (t, J = 5.9 Hz, NCH_2, 2H), 2.45 (br s, NH_2, 2H), 3.00 (t, J = 5.9 Hz, CH_2CO, 2H), 7.34 (br s, NH, 1H). ESI-MS: 487 $(M+1)^+$.

4.1.12. Fluorescein-5-thiocarbamoyl triester 17

Fluorescein isothiocyanate (2 mmol) was added to a solution of **16** (2 mmol) in DMF (20 mL). The reaction mixture was stirred for 24 h at room temperature. After evaporation, the residue was purified by column chromatography (eluent: MeOH/$CHCl_3$ = 1:9) to obtain an orange foam (78%). ^{1}H NMR ($CDCl_3$) δ: 1.40 (s, $C(CH_3)_3$, 27H), 1.95 (m, CH_2CH_2CO, 6H), 2.21 (m, CH_2CH_2CO, 6H), 2.55 (t, CH_2CO, J = 7.5 Hz, 2H), 3.93 (t, J = 7.5 Hz, NCH_2, 2H), 6.53–8.30 (m, ArH, 9H). ESI-MS: 876 $(M+1)^+$.

4.1.13. Fluorescein-5-thiocarbamoyl triacid 18

An analogous procedure described for **4** gave fluorescein-5-thiocarbamoyl triacid **18**. Mp 195–198 °C. ^{1}H NMR (DMSO-d_6) δ: 1.84–1.88 (m, CH_2CH_2CO, 6H), 2.11–2.16 (m, CH_2CH_2CO, 6H), 2.46 (t, J = 6.4 Hz, CH_2CO, 2H), 3.44 (q, J = 7.0 Hz, NCH_2, 2H), 6.53–8.32 (m, ArH, 9H), 10.01 (br s, NH, 2H). ESI-MS: 708 $(M+1)^+$.

4.1.14. Fluorescein-5-thiocarbamoyl tri-(3-benzoxy)pyridine-4-one 19

An analogous procedure described for **9** gave fluorescein-5-thiocarbamoyl tri-(3-benzoxy)pyridine-4-one **19.** Mp 198–200 °C. ^{1}H NMR (DMSO-d_6) δ: 1.81 (m, CH_2CH_2CO, 6H), 2.03 (m, CH_2CH_2CO, 6H), 2.24 (s, CCH_3, 9H), 2.41 (m, CH_2CO, 2H), 3.38 (s, NCH_3, 9H), 3.68 (m, NCH_2, 2H), 4.33 (s, CCH_2N, 6H), 5.06 (s, $PhCH_2O$, 6H), 6.18 (s, pyridinone C-5H, 3H), 6.54–8.38 (m, ArH, 24H), 10.15 (br s, NH, 1H), 10.27 (br s, NH, 1H). *m/z*: 1428 $(M+1)^+$. Elemental Anal. Calcd for $C_{79}H_{81}N_9O_{15}S{\cdot}CHCl_3$: C, 62.07; H, 5.34; N, 8.14. Found: C, 62.32; H, 5.58; N, 8.25.

4.1.15. Fluorescein-5-thiocarbamoyl tri-(3-hydroxy)pyridin-4-one 20

An analogous procedure described for **11** gave fluorescein-5-thiocarbamoyl tri-(3-hydroxy)pyridin-4-one **20**. Mp 202–205 °C. ^{1}H NMR (400 MHz, CD_3OD) δ: 2.03 (m, CH_2CH_2CO, 6H), 2.30 (m, CH_2CH_2CO, 6H), 2.42 (m, CH_2CO, 2H), 2.64 (br s, CCH_3 + CH_2CO, 11H), 3.89 (m, NCH_2, 2H), 4.02 (s, NCH_3, 9H), 4.74 (s, CCH_2N, 6H), 6.38–8.83 (m, ArH + pyridinone C-5H, 12H), 10.75 (br s, NH, 1H), 10.95 (br s, NH, 1H). ^{13}C NMR (100 MHz, CD_3OD) δ: 21.35 ($3CCH_3$), 30.85 ($3CCH_2CH_2$), 31.13 (CH_2CH_2CO), 31.26 ($3CCH_2CH_2$), 36.50 ($3NHCH_2$-pyridinone), 40.13 ($3NCH_3$), 41.85 ($NHCH_2CH_2$), 59.28 (C), 103.46 (CH), 103.57 (CH), 114.26 (3CH in pyridinone), 116.04 (C), 118.62 (CH), 129.77 (C), 130.29 (CH), 132.24 (C), 133.01 (CH), 135.27 (C), 140.99 (3C in pyridinone), 144.77 (3C in pyridinone), 150.88 (3C in pyridinone), 158.44 (C), 160.81 (C), 161.19 (3CO in pyridinone), 168.85 (C), 173.58 (C), 176.65 (C), 176.68 (3CONH), 182.54 (C). *m/z*: 1158 $(M+1)^+$. Elemental Anal. Calcd for $C_{59}H_{72}N_9O_{17}SCl_5$: C, 51.03; H, 5.23; N, 9.08. Found: C, 51.18; H, 5.48; N, 8.96.

4.2. Fluorescence measurements

The fluorescent intensity was scanned with either a Perkin–Elmer spectrofluorometer (type LS 50B) or a CytoFluor 4000 Fluorescence Multi-Well Plate Reader. Spectra were not corrected for light intensity or detector sensitivity. Data were recorded on-line and analysed by excel software on a PC. Fluorescence measurements were performed twice in MOPS buffer (50 mM, pH 7.4) at 22 °C and carried out independently at least three times on different days. The results are expressed as means ± SD.

Acknowledgement

Authors would like to thank Dr. Dingyong Liu for preparing the 'unknown' concentrations of iron samples.

Supplementary data

Supplementary data associated with this article can be found, in the online version, at doi:10.1016/j.bmc.2009.09.052.

References and notes

1. Bothwell, T. H.; Charlton, R. W.; Cook, J. D.; Finch, C. A. *Iron Metabolism in Man*; Blackwell Scientific: Oxford, 1979.
2. Crichton, R. R. *Inorganic Biochemistry of Iron Metabolism*; John Wiley & Sons: West Sussex, 2001.
3. Conrad, M. E.; Barton, J. C. *Am. J. Hematol.* **1981**, *10*, 199.
4. Chung, J.; Wessling-Resnick, M. *Crit. Rev. Clin. Lab. Sci.* **2003**, *40*, 151.
5. Anderson, G. J. *J. Gastroenterol. Hepatol.* **1999**, *14*, 105.
6. Breuer, W.; Hershko, C.; Cabantchik, Z. I. *Transfus. Sci.* **2000**, *23*, 185.
7. Jacobs, E. M. G.; Hendriks, J. C. M.; van Tits, B. L. J. H.; Evans, P. J.; Breuer, W.; Liu, D. Y.; Jansen, E. H. J. M.; Jauhiainen, K.; Sturm, B.; Porter, J. B.; Scheiber-Mojdehkar, B.; von Bonsdorff, L.; Cabantchik, Z. I.; Hider, R. C.; Swinkels, D. W. *Anal. Biochem.* **2005**, *341*, 241.
8. Kolb, A. M.; Smit, N. P.; Lentz-Ljuboje, R.; Osanto, S.; van, P. J. *Anal. Biochem.* **2009**, *385*, 13.
9. Sahlstedt, L.; Ebeling, F.; von, B. L.; Parkkinen, J.; Ruutu, T. *Br. J. Haematol.* **2001**, *113*, 836.
10. von Bonsdorff, L.; Lindeberg, E.; Sahlstedt, L.; Lehto, J.; Parkkinen, J. *Clin. Chem.* **2002**, *48*, 307.
11. Nuttall, K. L.; Gordon, W. H.; Ash, K. O. *Ann. Clin. Lab. Sci.* **1995**, *25*, 264.
12. Yokoi, K.; Kimura, M.; Itokawa, Y. *Biol. Trace Elem. Res.* **1991**, *31*, 265.
13. Gosriwatana, I.; Loreal, O.; Lu, S.; Brissot, P.; Porter, J.; Hider, R. C. *Anal. Biochem.* **1999**, *273*, 212.
14. Jakeman, A.; Thompson, T.; McHattie, J.; Lehotay, D. C. *Clin. Biochem.* **2001**, *34*, 43.
15. Jittangprasert, P.; Wilairat, P.; Pootrakul, P. *Southeast Asian J. Trop. Med. Public Health* **2004**, *35*, 1039.

16. von, B. L.; Tolo, H.; Lindeberg, E.; Nyman, T.; Harju, A.; Parkkinen, J. *Biologicals* **2001**, *29*, 27.
17. Breuer, W.; Cabantchik, Z. I. *Anal. Biochem.* **2001**, *299*, 194.
18. Breuer, W.; Ermers, M. J.; Pootrakul, P.; Abramov, A.; Hershko, C.; Cabantchik, Z. I. *Blood* **2001**, *97*, 792.
19. Breuer, W.; Ronson, A.; Slotki, I. N.; Abramov, A.; Hershko, C.; Cabantchik, Z. I. *Blood* **2000**, *95*, 2975.
20. O'Sullivan, B.; Xu, J.; Raymond, K. N. In *Iron chelators: new development strategies*, Badman, D. G., Bergeron, R. J., Brittenham, G. M., Eds.; Saratoga Publishing Group: Ponte Vedra, **2000**, pp 177–208.
21. Liu, Z. D.; Piyamongkol, S.; Liu, D. Y.; Khodr, H. H.; Lu, S. L.; Hider, R. C. *Bioorg. Med. Chem.* **2001**, *9*, 563.
22. Newkome, G. R.; Behera, R. K.; Moorefield, C. N.; Baker, G. R. *J. Org. Chem.* **1991**, *56*, 7162.
23. Ma, Y.; Luo, W.; Quinn, P. J.; Liu, Z.; Hider, R. C. *J. Med. Chem.* **2004**, *47*, 6349.
24. Liu, Z. D.; Hider, R. C. *Med. Res. Rev.* **2002**, *22*, 26.
25. Bino, A.; Shweky, I.; Cohen, S.; Bauminger, E. R.; Lippard, S. J. *Inorg. Chem.* **1998**, *37*, 5168.
26. Evans, R. W.; Rafique, R.; Zarea, A.; Rapisarda, C.; Cammack, R.; Evans, P. J.; Porter, J. B.; Hider, R. C. *J. Biol. Inorg. Chem.* **2008**, *13*, 57.
27. Faller, B.; Nick, H. *J. Am. Chem. Soc.* **1994**, *116*, 3860.
28. al-Refaie, F. N.; Wickens, D. G.; Wonke, B.; Kontoghiorghes, G. J.; Hoffbrand, A. V. *Br. J. Haematol.* **1992**, *82*, 431.
29. Chapman, J. M., Jr.; Cocolas, G. H.; Hall, I. H. *J. Med. Chem.* **1983**, *26*, 243.